Lawrence Berkeley National Laboratory

Title
THE ADSORPTION OF BENZENE ON THE Pt(lll) SURFACE STUDIED BY LOW-ENERGY ELECTRON DIFFRACTION INTENSITY MEASUREMENTS AND QUANTITATIVE AUGER ELECTRON SPECTROSCOPY

Permalink
https://escholarship.org/uc/item/04s1964s

Author
Stair, P.C.

Publication Date
1977-06-01

UC-4

LBL-6286 C·1
Preprint

THE ADSORPTION OF BENZENE ON THE Pt(111)
SURFACE STUDIED BY LOW-ENERGY ELECTRON
DIFFRACTION INTENSITY MEASUREMENTS AND
QUANTITATIVE AUGER ELECTRON SPECTROSCOPY

P. C. Stair and G. A. Somorjai

June 24, 1977

LBL-6286 C·1

DISCLAIMER

THE ADSORPTION OF BENZENE ON THE Pt(111) SURFACE STUDIED BY LOW-ENERGY ELECTRON DIFFRACTION INTENSITY MEASUREMENTS AND QUANTITATIVE AUGER ELECTRON SPECTROSCOPY
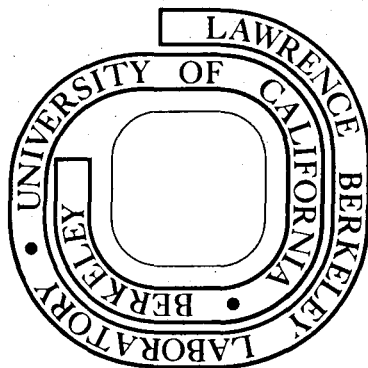
by

P. C. Stair and G. A. Somorjai

Materials and Molecular Research Division, Lawrence Berkeley Laboratory, Department of Chemistry, University of California Berkeley, California 94720

Abstract

Benzene, when chemisorbed on the Pt(111) crystal face forms an ordered metastable $\begin{vmatrix} 4 & -2 \\ 0 & 4 \end{vmatrix}$ surface structure which transforms, slowly, to a stable $\begin{vmatrix} 4 & -2 \\ 0 & 5 \end{vmatrix}$ surface structure. A complete set of intensity-voltage (I vs V) curves are presented in the appendix to aid in solving the surface structures of this complex organic molecule. The size of the unit cells and the larger than monolayer carbon surface concentrations (determined by quantitative Auger spectroscopy) indicate that most of the adsorbed benzene molecules are inclined at an angle to the surface. The similarity of the (I-V) profiles for the same diffraction beams from the two structures indicate that the carbon-platinum layer spacing changes very little during the order-order transformation.

Introduction

The adsorption of benzene on the platinum (111) surface was studied by Gland and Somorjai using work function change and low-energy electron diffraction (LEED) measurements.[1,2] Two ordered benzene adsorbate structures were found and characterized by work function and LEED pattern changes. Adsorption at room temperature with a benzene pressure of 4×10^{-7} torr initially gave a work function change of -1.4 volts and a diffraction

pattern analyzed as three domains of a rectangular $\begin{vmatrix} 4 & -2 \\ 0 & 4 \end{vmatrix}$ structure.[3]
After continued exposure to benzene vapor for ∿40 minutes, the work function
change was -0.7 volts and the surface structure had transformed into three
domains of a structure analyzed as $\begin{vmatrix} 4 & -2 \\ 0 & 5 \end{vmatrix}$.[4] The diffraction patterns
and real space surface structures are shown in Figs. 1, 2, 3 and 4.

Finding the location of the adsorbed benzene molecules with respect
to the position of the platinum atoms in the surface and relative to their
neighboring benzene molecules is the goal of surface structure analysis
utilizing the intensities of the diffraction beams obtained at various
electron energies. In this paper we report the complete set of intensity
vs incident electron beam energy (I-V) curves for both the metastable
$\begin{vmatrix} 4 & -2 \\ 0 & 4 \end{vmatrix}$ and the stable $\begin{vmatrix} 4 & -2 \\ 0 & 5 \end{vmatrix}$ benzene structures. These LEED intensity
measurements are an extension of our studies to determine the structure
of small hydrocarbons adsorbed on the platinum (111) surface.[6] We hope
that by making the intensity profiles generally available, we shall stim-
ulate theoretical interest in solving the more complex adsorbate struc-
tures of larger hydrocarbon molecules.

We also present additional observations and analysis of the benzene
transformation that should aid the determination of the benzene adsorbate
structure and bonding. We observed the benzene structural transformation
occuring in ∿3 1/2 hours at room temperature in vacuum or in ∿50 minutes
at a pressure of 1×10^{-7} torr benzene in agreement with the results of
Gland and Somorjai. We also observed that gentle heating of the meta-
stable benzene $\begin{vmatrix} 4 & -2 \\ 0 & 4 \end{vmatrix}$ structure in vacuum increased the transformation
rate to completion in ∿50 minutes and that the transformation was charact-
erized by continuous splitting of some of the LEED beams similar to that

observed for oxygen adsorbed on Ni(110).[5] The measured intensities indicate that very little change in the perpendicular platinum-carbon layer spacing accompanies the benzene structural transformation. Both the size of the benzene unit cells[1] and the calibrated determination of the carbon content in the benzene structures strongly suggest that neither structure represent a uniform, π-coordinate configuration but that benzene adsorbs with the plane of the benzene ring inclined at an angle to the surface.

Experimental

The ultrahigh vacuum LEED/Auger apparatus and photographic intensity measurement technique have been described in detail elsewhere.[6,7,8] Matheson Spectroquality benzene was used without further purification except for degassing by a series of freeze-pump-thaw cycles.

The (111) surface was prepared for benzene adsorption and LEED intensity measurements following a standard procedure which has been previously described.[6] The benzene adsorption onto the clean Pt(111) surface was carried out at a surface temperature of 300 K in a benzene pressure of 1×10^{-7} torr. An exposure of ~ 70 L $= 7 \times 10^{-5}$ torr-sec gave a well ordered benzene LEED pattern characteristic of a metastable $\begin{vmatrix} 4 & -2 \\ 0 & 4 \end{vmatrix}$ surface structure (see Figs. 1 and 2). After pumping out the sample region to a base pressure of $\sim 1 \times 10^{-9}$ torr, this initial benzene structure transformed slowly into a stable $\begin{vmatrix} 4 & -2 \\ 0 & 5 \end{vmatrix}$ structure over a period of 3 1/2 hours (see Figs. 3 and 4). By maintaining the benzene pressure at 1×10^{-7} torr or by heating the sample to 325 K following evacuation to 1×10^{-9} torr, the benzene structural transformation rate increased so that the change was completed within 50 minutes. Heating the sample above 350 K disordered

the benzene overlayer. These observations are in complete agreement with the work of Gland and Somorjai but with the additional result that the transformation rate is sensitive to the sample temperature.

The LEED intensity vs voltage curves for both benzene structures were measured photographically from 10 eV to 100 eV in 2 eV intervals using 1/2 second exposures at f1.8. Above 100 eV some of the diffraction beams are so close together that their separate intensities cannot be resolved. The incident electron beam current was measured following each series of photographs for purposes of normalizing the intensities to 1 μ-amp. The incident current varied from ∿0.04 μ-amp at 10 eV to ∿1 μ-amp at 100 eV giving a total electron beam exposure of ∿11 μ-amp-sec-mm^{-2}. The reduction in the benzene overlayer LEED intensity during the measurement due to electron beam effects was estimated for both benzene structures by measuring the rate of LEED intensity decay with beam exposure. Intensity reductions of 2% and 13% were found for the metastable $\begin{vmatrix} 4 & -2 \\ 0 & 4 \end{vmatrix}$ and the stable $\begin{vmatrix} 4 & -2 \\ 0 & 5 \end{vmatrix}$ structures respectively. The reduction of LEED pattern photographs to intensity vs energy curves has been described in detail elsewhere.[6,7,8]

The carbon (272 eV)/platinum (237 eV) Auger peak ratios were measured using the retarding field LEED/Auger analyzer in order to determine the change in surface carbon content on going from the $\begin{vmatrix} 4 & -2 \\ 0 & 4 \end{vmatrix}$ to the $\begin{vmatrix} 4 & -2 \\ 0 & 5 \end{vmatrix}$ structure. The primary electron beam energy was 2500 eV with an incident current of ∿60 μ-amp. The spectrum was recorded in the dN(E)/dE mode, and the resulting first derivative peak-to-peak height was taken as the measure of Auger intensity. The carbon/platinum Auger peak ratios were compared to the identical measurements performed on ordered (2x2) struc-
tures of acetylene, ethylene, propylene and methylacetylene adsorbed on

the Pt(111) surface in order to determine the concentration of carbon on the surface.

Results

A.   Intensity Measurements

The diffraction intensities from both benzene structures were measured at normal incidence and at polar angles, $\theta \pm 0.1°$, of 4°, 10° and 16° all at an azimuthal angle $\phi = 0$. The polar and azimuthal angles are defined according to Jona's convention.[9] The intensities are presented in the appendix in the usual form of normalized intensity vs incident electron beam energy (I-V curves). (The intensities may also be obtained in numerical form if desired by direct communication with the authors.)

While a large number of diffraction beams are within the camera field of view at one time, most of these are either too dim to be detected by the film or they are detected only within a very narrow energy range. Only the brightest diffraction beams are reported. The I-V curves in the appendix are identified with particular beams in the diffraction pattern via the arbitrary numerical labels in Figs. 2 and 4. The diffraction beams arising from the platinum substrate are identified by the usual Miller Index notation. The reproducibility of the I-V curves was checked after ion sputtering and oxygen cleaning of the crystal surface. The repeat measurements are shown as the dotted curves on the I-V plots. The intensity scales are in arbitrary units, but the same units are used for all the curves, and each curve has been normalized to a constant beam current of 1 μ-amp. Gaps in the curves occur whenever the spot intensity falls below the threshold of the film. In addition, the ($\bar{1}0$) beam at $\theta = 10°$ is

blocked from view above 76 eV by the sample holder. The benzene $\begin{vmatrix} 4 & -2 \\ 0 & 4 \end{vmatrix}$ beams labeled 1, 4 and 5 are equivalent at normal incidence by symmetry as are beams 2, 3 and 6 (see Fig. 2). There are three sets of equivalent beams for the $\begin{vmatrix} 4 & -2 \\ 0 & 5 \end{vmatrix}$ structure at normal incidence: these are labeled 1, 5, 7 and 2, 4, 8 and 3, 6, 9 in Fig. 4. The structure in these curves consists mainly of a series of small shoulders that are barely resolved. However, the energy positions of these features agree well for equivalent beams indicating that the shoulders are simply noise. The best agreement is between beams which result from the same benzene domain, i.e., 1, 4 and 3, 6 for structure $\begin{vmatrix} 4 & -2 \\ 0 & 4 \end{vmatrix}$; 1, 5 and 4, 8 for structure $\begin{vmatrix} 4 & -2 \\ 0 & 5 \end{vmatrix}$ (see Figs. 2 and 4).

B. Adsorption and Transformation

The diffraction patterns characteristic of the $\begin{vmatrix} 4 & -2 \\ 0 & 4 \end{vmatrix}$ and $\begin{vmatrix} 4 & -2 \\ 0 & 5 \end{vmatrix}$ benzene structures are shown diagramatically in Figs. 2 and 4 respectively. These patterns are formed by three domains of the rectangular unit cells given by the matrix notation. These unit cells are shown in Figs. 1 and 3 along with photographs of the LEED pattern and a diagram of the benzene molecule including van der Waals radii. The reciprocal space unit cells are indicated in Figs. 2 and 4.

The benzene adsorbate transformation involves an expansion of the rectangular unit cell in one dimension, extending the long side of the unit cell. The transformation rate depends on both the sample temperature and the pressure of benzene in the vapor phase above the crystal surface as described above. Under conditions where the transformation is slowest (crystal temperature $\sim$300 K, pressure $\sim$1x10^{-9} torr) the diffraction pattern exhibits continuous splitting of some of the diffraction beams at inter-

mediate stages of the transformation. This is analogous to the observations of Germer, May and Szostak for oxygen adsorption on Ni(110).[5] The arrows in Fig. 2 indicate which of the spots in the initial $\begin{vmatrix} 4 & -2 \\ 0 & 4 \end{vmatrix}$ structure undergo splitting. Spot 8 in Fig. 2, for example, splits into five spots with the direction of the spot splitting indicated by the arrows. The five spots which result from the splitting of spot 8 are spot 11 in Fig. 4 and its four nearest neighbors. The direction of the spot splitting parallels the direction of the expansion from the $\begin{vmatrix} 4 & -2 \\ 0 & 4 \end{vmatrix}$ unit cell to the $\begin{vmatrix} 4 & -2 \\ 0 & 5 \end{vmatrix}$ unit cell. This is seen more clearly for a single domain of the benzene adsorbate as shown in Fig. 5. Referring to Fig. 5, the spots in rows $\underline{a}$ split into two spots. The row $\underline{b}$ spots move but remain unsplit, and the rest of the spots remain stationary. The explanation for this behavior as given by Germer, May and Szostak and later verified by Park and Houston[10] is that at intermediate stages in the transformation the overlayer must contain both unit cells within an ordered domain and that the unit cells must be mixed randomly. The splitting progresses as a larger fraction of the surface is covered by the $\begin{vmatrix} 4 & -2 \\ 0 & 5 \end{vmatrix}$ unit cell. In future work it should be possible to determine the kinetics of the transformation from careful observation of the evolving LEED pattern.

C. Surface Carbon Content

If we assume that the shape of the peaks in the Auger N(E) spectrum do not change with carbon coverage, the amount of carbon on the surface may be determined from the peak-to-peak height in the first derivative Auger spectrum, dN(E)/dE. The measurement may be made independent of the incident electron beam current and the Auger electron analyzer tuning by taking the ratio of the carbon Auger peak to a platinum Auger peak as the

measure of carbon content. The carbon (272 eV)/platinum (237 eV) peak ratio was used as the measure of the surface carbon in this work.

A quantitative calibration of the C/Pt ratio was obtained using the acetylene-Pt(111)-(2x2) structure assuming one acetylene molecule per (2x2) unit cell. Using a platinum-platinum distance of 2.77 $\overset{\circ}{A}$ gives an area for the (2x2) unit cell of 26.6 $\overset{\circ}{A}{}^2$ since acetylene contains two carbon atoms this corresponds to 1/2 monolayer of carbon and 0.075 C atoms/$\overset{\circ}{A}{}^2$. A variety of observations indicate that this should be an accurate calibration. Dynamical LEED intensity calculations have definitely shown that the acetylene overlayer is composed of one acetylene molecule per (2x2) unit cell and not three domains of a (2x1) structure.[11] The acetylene (2x2) structure formed only within a very narrow exposure range with a 10% overexposure eliminating the (2x2) structure and 10% underexposure resulting in only a poorly formed (2x2) structure.[6] This implies that the (2x2) structure occurs only over a narrow coverage range. This is also consistent with the reproducibility of the acetylene (2x2) C/Pt Auger peak ratio which was within 3% from one adsorption study to another. Finally, the ethylene-Pt(111)-(2x2) adsorbate yielded the same C/Pt Auger ratio as acetylene while the (2x2) structures of methylacetylene and propylene gave Auger ratios 50% larger, all consistent with one molecule adsorbed per (2x2) unit cell and demonstrating the validity of the ratio method of determining surface carbon content.

The Auger measurements for both benzene structures were taken in a background pressure of 1×10^{-9} torr, with the benzene flux shut off. However, the stable $\left| \begin{matrix} 4 & -2 \\ 0 & 5 \end{matrix} \right|$ benzene structure was prepared from the meta-stable $\left| \begin{matrix} 4 & -2 \\ 0 & 4 \end{matrix} \right|$ structure under conditions of 1×10^{-7} torr benzene pressure.

Using the acetylene calibration, the surface carbon concentration in the two benzene structures was: $\left|\begin{smallmatrix} 4 & -2 \\ 0 & 4 \end{smallmatrix}\right|$: 0.37 C atoms/$\mathring{A}^2 \pm 0.06$; $\left|\begin{smallmatrix} 4 & -2 \\ 0 & 5 \end{smallmatrix}\right|$: 0.46 C atoms/$\mathring{A}^2 \pm 0.03$. For comparison, a monolayer of carbon on Pt(111) would correspond to 0.15 C atoms/$\mathring{A}^2$.

Discussion

The purpose of this paper is to present an extensive set of low-energy electron diffraction intensity vs energy curves for both metastable and stable ordered structures of benzene adsorbed on the platinum (111) crystal face in order that this data may be generally available to all workers in the field. Work function and Auger measurements that provide further information on the nature of the adsorbate structures are also discussed. The transformation from the metastable $\left|\begin{smallmatrix} 4 & -2 \\ 0 & 4 \end{smallmatrix}\right|$ benzene structure to the stable $\left|\begin{smallmatrix} 4 & -2 \\ 0 & 5 \end{smallmatrix}\right|$ benzene structure was studied only to the extent necessary to obtain the best quality diffraction patterns. Future studies of the changes in the LEED pattern will provide information on the kinetics of the transformation.

It is important to note that many hydrocarbons chemisorbed on the platinum (111) surface commonly give multiple adsorption states. This has been observed for acetylene,[6,8,15,16,17,18] methylacetylene,[6,8] ethylene[18] and benzene[1] by LEED pattern changes,[1] LEED intensity changes,[6,8,15] ultraviolet photoelectron spectroscopy[16,17] and electron loss spectroscopy.[18] These multiple adsorption stages suggest that the type of chemical bonding between the platinum (111) substrate and a given hydrocarcon adsorbate may take a variety of forms, depending on surface temperature and coverage. The presence of multiple binding sites and/or binding states

indicate that this "flat" and structurally "uniform" surface is very heterogeneous as seen by the hydrocarbon molecules. It appears that multiple binding sites and/or binding states may be a general property of hydrocarbons on platinum surfaces and perhaps on other metal surfaces as well.

In fact, multiple benzene monolayer structures have been observed on the silver (111) crystal face depending on the surface temperature and benzene exposure.[19] A $(2\sqrt{3}x2\sqrt{3})$ R30° structure has also been reported for low exposures of benzene on Ni(111). The adsorption of benzene into this ordered nickel adsorbate was irreversible. Further benzene exposure led to a reversibly adsorbed component.[20] The chemisorption of benzene on the Ir(111) surface at 300°C, however, already leads to partial decomposition and to the formation of a poorly ordered (3x3) surface structure;[21] on heating to 500°C or above, complete disordering and decomposition occurs.

A. Intensities

Without complete dynamical analysis, the LEED intensities from the benzene overlayers can give little information on the overlayer structure. However, the changes observed in the I-V curves for the beams common to both structures when compared to the changes observed for the two ordered (2x2) acetylene structures on Pt(111) suggest, as discussed below, that the carbon-platinum perpendicular layer spacing is nearly the same for both benzene structures.

Acetylene was found, just as benzene, to adsorb into two ordered structures, metastable and stable, on the platinum (111) surface.[6,15] The structures were distinguishable by their LEED intensities, and the

dramatic changes observed were ascribed mainly to a change in the carbon-platinum perpendicular layer spacing.[12] In the energy range most sensitive to the hydrocarbon overlayer, below 100 eV, the acetylene structural transformation led to significant changes in the LEED intensity profiles for both the integral and fractional order beams. The benzene structural transformation does not cause changes in the intensity profiles of the magnitude seen for acetylene.

In order to consider intensity changes between the two benzene structures, we must examine diffraction beams which occur in both LEED patterns. The integral order beams and beams 7 and 8 in structure $\begin{vmatrix} 4 & -2 \\ 0 & 4 \end{vmatrix}$ (see Fig. 2) which correspond to 10 and 11 in structure $\begin{vmatrix} 4 & -2 \\ 0 & 5 \end{vmatrix}$ (see Fig. 4), are examples of such diffraction beams. The intensity profiles for the integral order beams are nearly identical for both benzene structures. In addition, when spots 7 and 8 in structure $\begin{vmatrix} 4 & -2 \\ 0 & 4 \end{vmatrix}$ (see Fig. 2) split into spots 10 and 11 and their four nearest neighbors in structure $\begin{vmatrix} 4 & -2 \\ 0 & 5 \end{vmatrix}$ (see Fig. 4), the spots which don't move during the transformation, i.e., 10 and 11, have nearly the same I-V curves as the original spots in $\begin{vmatrix} 4 & -2 \\ 0 & 4 \end{vmatrix}$, i.e., 7 and 8 (see appendix). Since dramatic changes in the I-V curves are associated mainly with changes in the spacing of atomic layers perpendicular to the surface[12] as occurred in the acetylene transformation, these observations suggest that such spacing changes are not occurring in the benzene transformation.

B. Auger Spectra, Work Function Measurements and the Benzene Adsorbate
    Structures

Two popular models for the bonding of benzene to a metal surface are the π-coordinate bonding with the plane of the benzene parallel to the

(that involves the removal of hydrogen from the molecule)
metal surface and a σ-type dissociative bonding/through one of the ring
carbons with the plane of the ring inclined at an angle with respect to
the surface.[13] In addition to the LEED patterns reported here, Gland and
Somorjai[1] also observed rather different work function changes with respect
to the clean (111) surface for the two structures: -1.4 volts for the
$\begin{vmatrix} 4 & -2 \\ 0 & 4 \end{vmatrix}$ structure and -0.7 volts for the $\begin{vmatrix} 4 & -2 \\ 0 & 5 \end{vmatrix}$ structure. They inter-
preted these quite different work function changes as an indication that
the benzene-metal bonding changed from π-coordinate in the $\begin{vmatrix} 4 & -2 \\ 0 & 4 \end{vmatrix}$ struc-
ture to σ-type in the $\begin{vmatrix} 4 & -2 \\ 0 & 5 \end{vmatrix}$ structure.

It is difficult to reconcile the large difference in work function
change between the two benzene structures with the negligible changes ob-
served in the I-V curves. The former certainly suggest a change in the
bonding between the overlayer and the metal substrate while the latter
indicate that this must occur without perturbing the overlayer-substrate
spacing.

The surface carbon concentration for the two structures determined
by calibrated Auger measurements strongly indicate that both benzene
structures must have some of the benzene molecules with the ring inclined
at an angle to the surface implying σ-type bonding. The measured carbon
concentrations are $\begin{vmatrix} 4 & -2 \\ 0 & 4 \end{vmatrix}$- 0.37 C atoms/$\text{Å}^2$±0.06 and $\begin{vmatrix} 4 & -2 \\ 0 & 5 \end{vmatrix}$ 0.46 C atoms/Å^2
±0.03. For a purely π-coordinated benzene structure with the ring
parallel to the surface, the closest packing arrangement for a single
layer in the $\begin{vmatrix} 4 & -2 \\ 0 & 4 \end{vmatrix}$ structure is shown in Fig. 6. The size of the benzene
includes the appropriate van der Waal's radii. This proposed structure has
a carbon concentration of 0.11 C atoms/Å^2, less than 1/3 the measured
concentration. Clearly this geometry for the benzene molecule cannot

provide enough carbon unless a multilayer structure is formed. A multi-

layer structure is not likely at UHV pressures since the benzene-benzene

interactions are weak. The benzene-metal interactions are short range and

should not extend beyond one adsorbate layer.[3] The carbon concentration

in the most densely packed plane of solid benzene is higher than in the

π-coordinate structure with a carbon concentration of .22 C atoms/$\overset{\circ}{A}^2$ Pt(111).

Closest packing the benzene with the ring perpendicular to the surface

increases the carbon concentration further. Taking into account the van

der Waal's radii shown in Figs. 1 and 3, this structure gives a carbon

concentration of 0.31 C atoms/$\overset{\circ}{A}^2$ in reasonable agreement with the experi-

mental value.

While the experimental Auger carbon concentration suggests that the

benzene ring lies perpendicular to the surface, the measurements are

certainly not sufficient to prove this. Further checks of the carbon

Auger calibration need to be made using adsorbates where the carbon is

located in more than a single plane. In addition, the analysis neglects

peak ratios which have been shown to be important in interpreting Auger[4]

matrix and attenuation effects on the Auger/data from alloy surfaces

and may be important for carbon structures with multiple carbon planes.

Thus, for example, the Auger signal from the platinum substrate might be

significantly attenuated passing through a thick carbon adsorbate relative

to the single carbon layer giving an anomalously large C/Pt Auger ratio.

In fact, the most densely packed benzene structure possible is with the

ring perpendicular to the surface yet the calculated carbon concentration

for this structure is still below the measured value. It is clear from

all of the available experimental evidence (surface unit cell size, surface

carbon concentration determined by AES and work function changes) that

some if not all of the adsorbed benzene molecules are inclined at an angle to the surface. However, we cannot say what the angle of inclination is or what fraction of the molecules is in this binding state.

Conclusion

Benzene adsorbs on the platinum (111) crystal face into a well-ordered metastable $\begin{vmatrix} 4 & -2 \\ 0 & 4 \end{vmatrix}$ structure at room temperature and ultrahigh Vacuum conditions. This initial structure transforms into a stable $\begin{vmatrix} 4 & -2 \\ 0 & 5 \end{vmatrix}$ structure at a rate which is sensitive both to the sample temperature and to the background benzene pressure. The LEED intensities indicate very little change in the carbon-platinum layer spacing accompanies the transformation yet the work function change suggests that the adsorbate-metal bonding is significantly different for the two structures. Both the surface unit cell size and the calibrated Auger determination of the surface carbon content indicate that the adsorbate structure must have some of the benzene molecules inclined at an angle to the surface.

In the absence of surface structure analysis we cannot identify the precise location of the benzene molecules with respect to each other or relative to the surface platinum atoms. However, the complete set of I-V curves presented here should be sufficient data-base for structure analysis.

Acknowledgment

References

1. J. L. Gland and G. A. Somorjai, Surf. Sci. $\underline{38}$, 157 (1973).

2. J. L. Gland and G. A. Somorjai, Adv. in Coll. and Int. Sci. $\underline{5}$, 205 (1976).

3. For a discussion of surface structure notation see G. A. Somorjai, Principles of Surface Chemistry, (Prentice-Hall, New Jersey, 1972).

4. In the first paper (Ref. 1) the unit cells of the benzene surface structure were reported erroneously. This was rectified by L. L. Kesmodel and was corrected in a subsequent publication (Ref. 4).

5. L. H. Germer, J. W. May and R. J. Szostak, Surf. Sci. $\underline{8}$, 430 (1967).

6. P. C. Stair and G. A. Somorjai, J. Chem. Phys. $\underline{66}$, 2036 (1977).

7. P. C. Stair, T. J. Kaminska, L. L. Kesmodel and G. A. Somorjai, Phys. Rev. B $\underline{11}$, 630 (1975).

8. P. C. Stair, Ph.D. Thesis, Department of Chemistry, University of California, Berkeley, 1977.

9. F. Jona, IBM J. Res. Div. $\underline{14}$, 444 (1970).

10. R. S. Park and J. E. Houston, Surf. Sci. $\underline{21}$, 209 (1970).

11. L. L. Kesmodel, P. C. Stair, R. C. Baetzold and G. A. Somorjai, Phys. Rev. Lett. $\underline{36}$, 1316 (1976).

12. L. L. Kesmodel, R. C. Baetzold and G. A. Somorjai, Surf. Sci., in press.

13. R. B. Mayes and P. B. Wells, Adv. in Catal. $\underline{23}$, 123 (1974).

14. S. H. Overbury and G. A. Somorjai, J. Chem. Phys. $\underline{66}$, 3181 (1977).

15. P. C. Stair and G. A. Somorjai, Chem. Phys. Lett. $\underline{41}$, 391 (1976).

16. W. J. Lo, Y. W. Chung, L. L. Kesmodel, P. C. Stair and G. A. Somorjai, Solid State Commun., in press.

17. J. E. Demuth, Chem. Phys. Lett. <u>45</u>, 12 (1977).

18. H. Ibach, H. Hopster and B. Sexton, to be published.

19. L. E. Firment, Ph.D. Thesis, Department of Chemistry, University of California, Berkeley, 1977.

20. G. Dalmai-Imelik and J. C. Bertolini, J. Vac. Sci. and Technol. <u>9</u>, 677 (1972).

21. B. E. Nieuwenhuys, D. I. Hagen, G. Rovida and G. A. Somorjai, Surf. Sci. <u>59</u>, 155 (1976).

Figure Captions

Fig. 1   A diffraction pattern resulting from the Pt(111)-$\begin{vmatrix} 4 & -2 \\ 0 & 4 \end{vmatrix}$-benzene

structure with a schematic diagram of the unit cell. The benzene

molecule including van der Waals radii is shown for comparison.

All lengths are in Angströms.

Fig. 2   A schematic diagram of the Pt(111)-$\begin{vmatrix} 4 & -2 \\ 0 & 4 \end{vmatrix}$-benzene diffraction

pattern. The orientation of the three rectangular domains is

shown. The numerical labels designate the diffraction spots for

which I-V profiles have been recorded. The arrows indicate the

movement of the spots during the transformation to the Pt(111)-

$\begin{vmatrix} 4 & -2 \\ 0 & 5 \end{vmatrix}$-benzene structure. The azimuthal angle, ϕ, is defined

according to reference 1.

Fig. 3   Diffraction patterns for the Pt(111)-$\begin{vmatrix} 4 & -2 \\ 0 & 5 \end{vmatrix}$-benzene structure

and a schematic diagram of the unit cell. The benzene molecule

including van der Waals radii is shown for comparison. All

lengths are in Angströms.

Fig. 4   A schematic diagram of the Pt(111)-$\begin{vmatrix} 4 & -2 \\ 0 & 5 \end{vmatrix}$-benzene diffraction

pattern. The orientation of the three rectangular domains is

shown. The numerical labels designate the diffraction spots

for which I-V profiles have been recorded. The azimuthal angle,

ϕ, is defined according to reference 1.

Fig. 5   A schematic diagram of one domain of the Pt(111)-$\begin{vmatrix} 4 & -2 \\ 0 & 4 \end{vmatrix}$-benzene

diffraction pattern. The arrows show the movement of the spots

during the transformation to the Pt(111)-$\begin{vmatrix} 4 & -2 \\ 0 & 5 \end{vmatrix}$-benzene struc-

ture. In rows (a) the spots split. In rows (b) the spots move

but do not split.

Fig. 6   A schematic diagram of the Pt(111)-$\begin{vmatrix} 4 & -2 \\ 0 & 4 \end{vmatrix}$-benzene unit cell

showing the closest packing of benzene with the plane of the
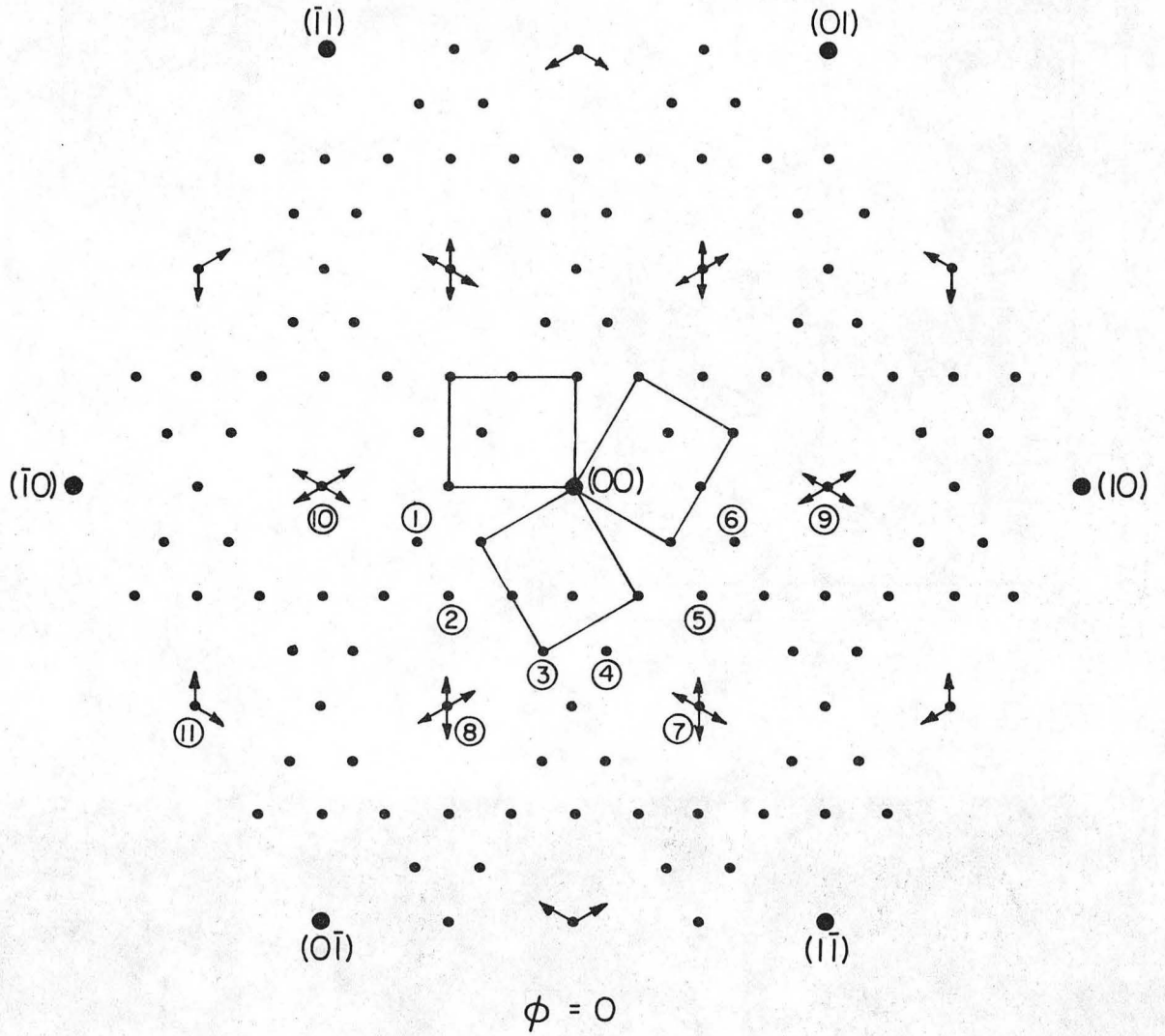
ring parallel to the surface.

-19-

Appendix

Fig. 1-G1. I-V profiles from the $\begin{vmatrix} 4 & -2 \\ 0 & 4 \end{vmatrix}$ benzene structure at normal incidence.

Fig. 1-G2. I-V profiles from the $\begin{vmatrix} 4 & -2 \\ 0 & 4 \end{vmatrix}$ benzene structure at $\theta=4°$.

Fig. 1-G3. I-V profiles from the $\begin{vmatrix} 4 & -2 \\ 0 & 4 \end{vmatrix}$ benzene structure at $\theta=10°$.

Fig. 1-G4. I-V profiles from the $\begin{vmatrix} 4 & -2 \\ 0 & 4 \end{vmatrix}$ benzene structure at $\theta=16°$.

Fig. 1-G5. I-V profiles from the $\begin{vmatrix} 4 & -2 \\ 0 & 5 \end{vmatrix}$ benzene structure at normal incidence.

Fig. 1-G6. I-V profiles from the $\begin{vmatrix} 4 & -2 \\ 0 & 5 \end{vmatrix}$ benzene structure at $\theta=4°$.

Fig. 1-G7. I-V profiles from the $\begin{vmatrix} 4 & -2 \\ 0 & 5 \end{vmatrix}$ benzene structure at $\theta=10°$.

Fig. 1-G8. I-V profiles from the $\begin{vmatrix} 4 & -2 \\ 0 & 5 \end{vmatrix}$ benzene structure at $\theta=16°$.

Pt(III) $- \begin{vmatrix} 4\hat{a} & -2\hat{b} \\ 0 & 4\hat{b} \end{vmatrix} -$ Benzene
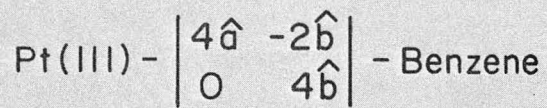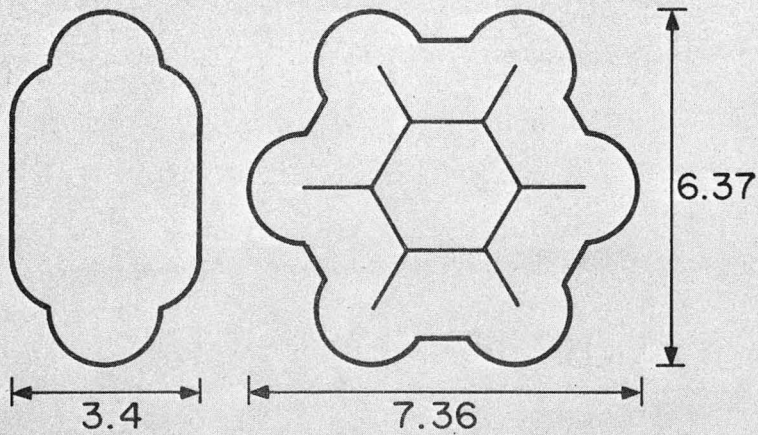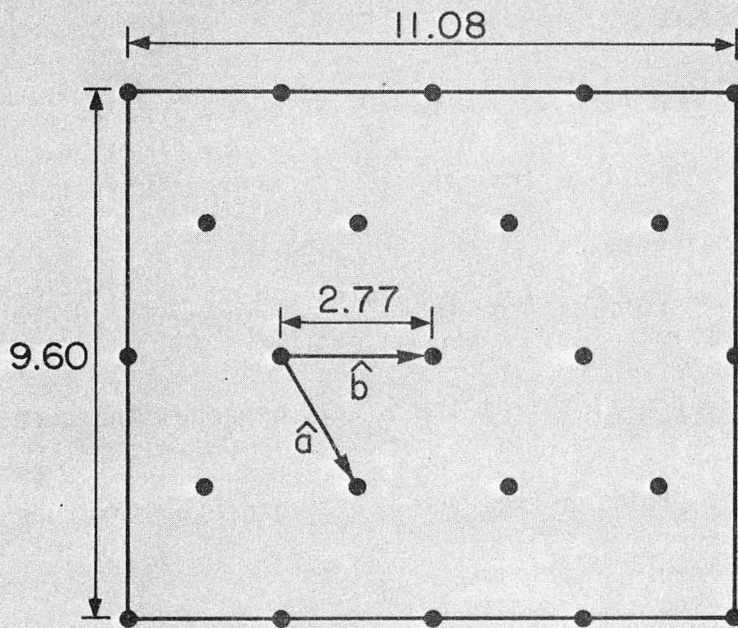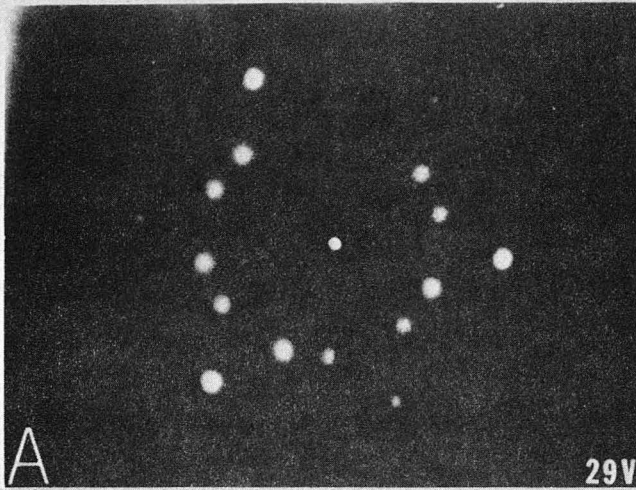
XBB 732-667A

Fig. 1

Benzene $\begin{pmatrix} 4 & -2 \\ 0 & 4 \end{pmatrix}$

$\phi = 0$

XBL 774-5256

Fig. 2

-22-

$$Pt(III) - \begin{vmatrix} 4\hat{a} & -2\hat{b} \\ 0 & 5\hat{b} \end{vmatrix} - Benzene$$
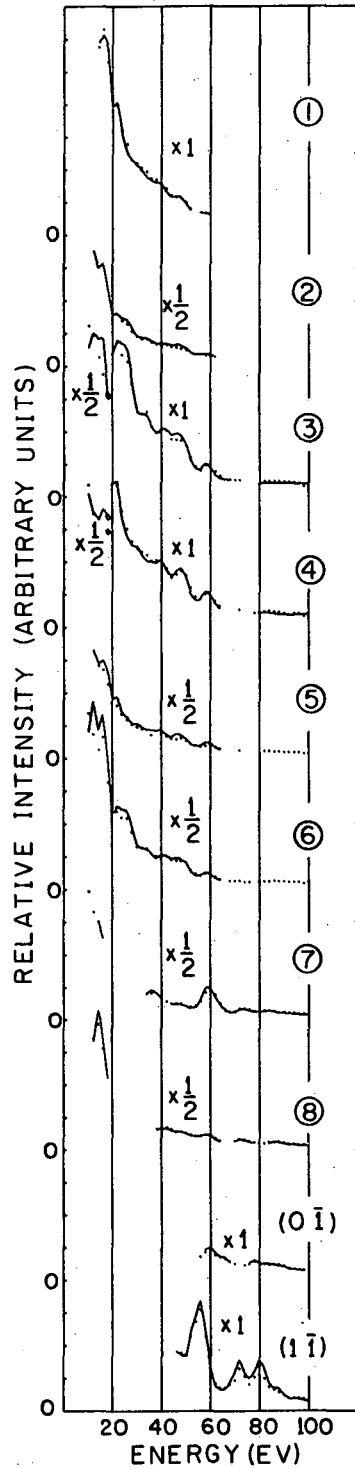
Fig. 3

XBB 732-663A

BENZENE $\begin{pmatrix} 4 & -2 \\ 0 & 5 \end{pmatrix}$

$\phi = 0$
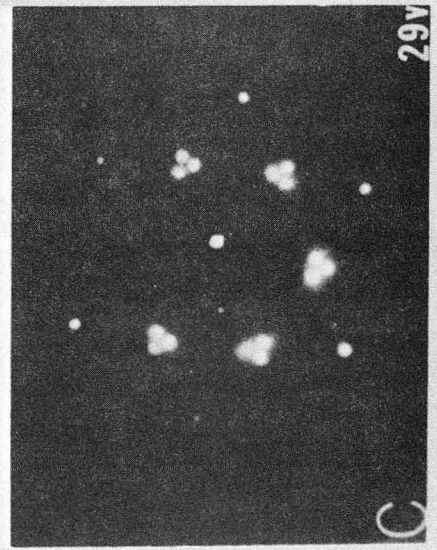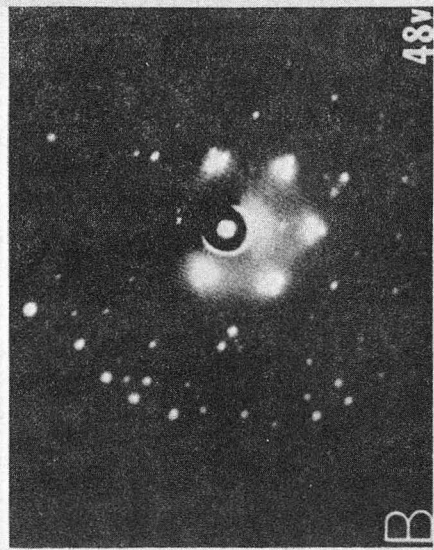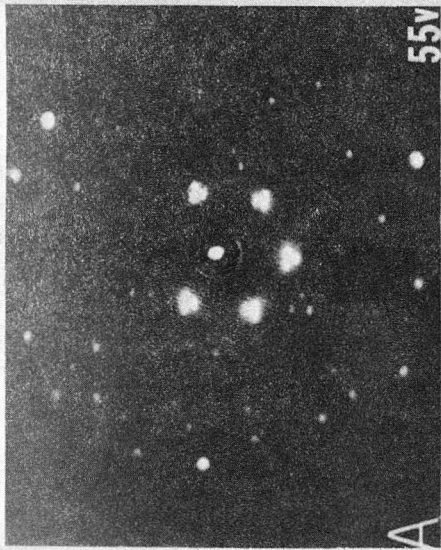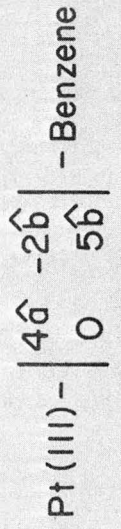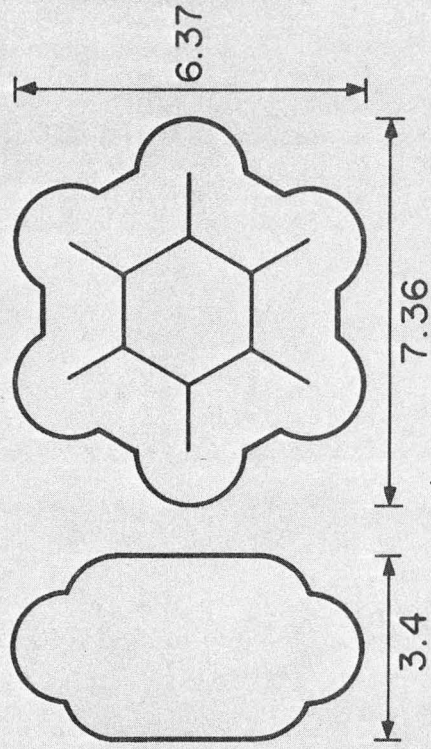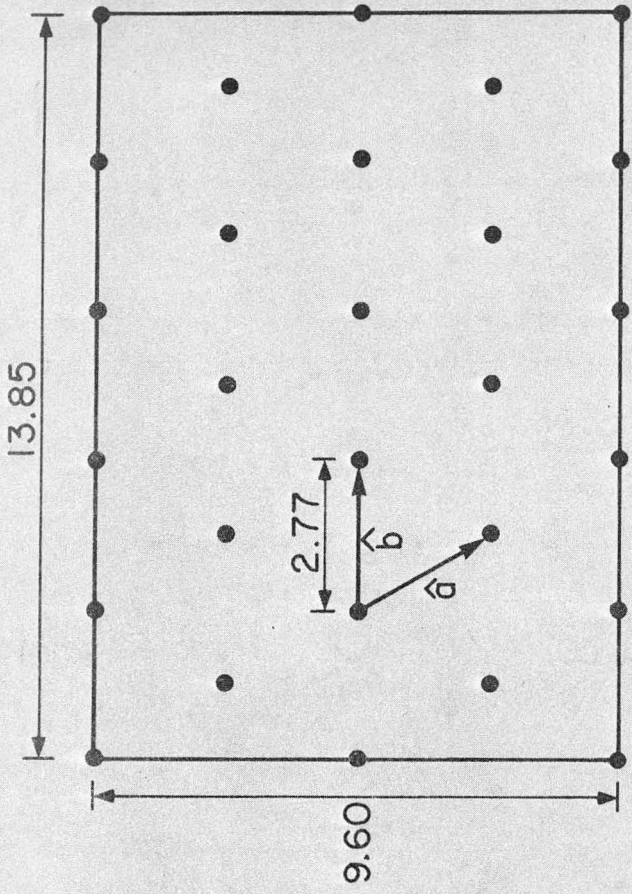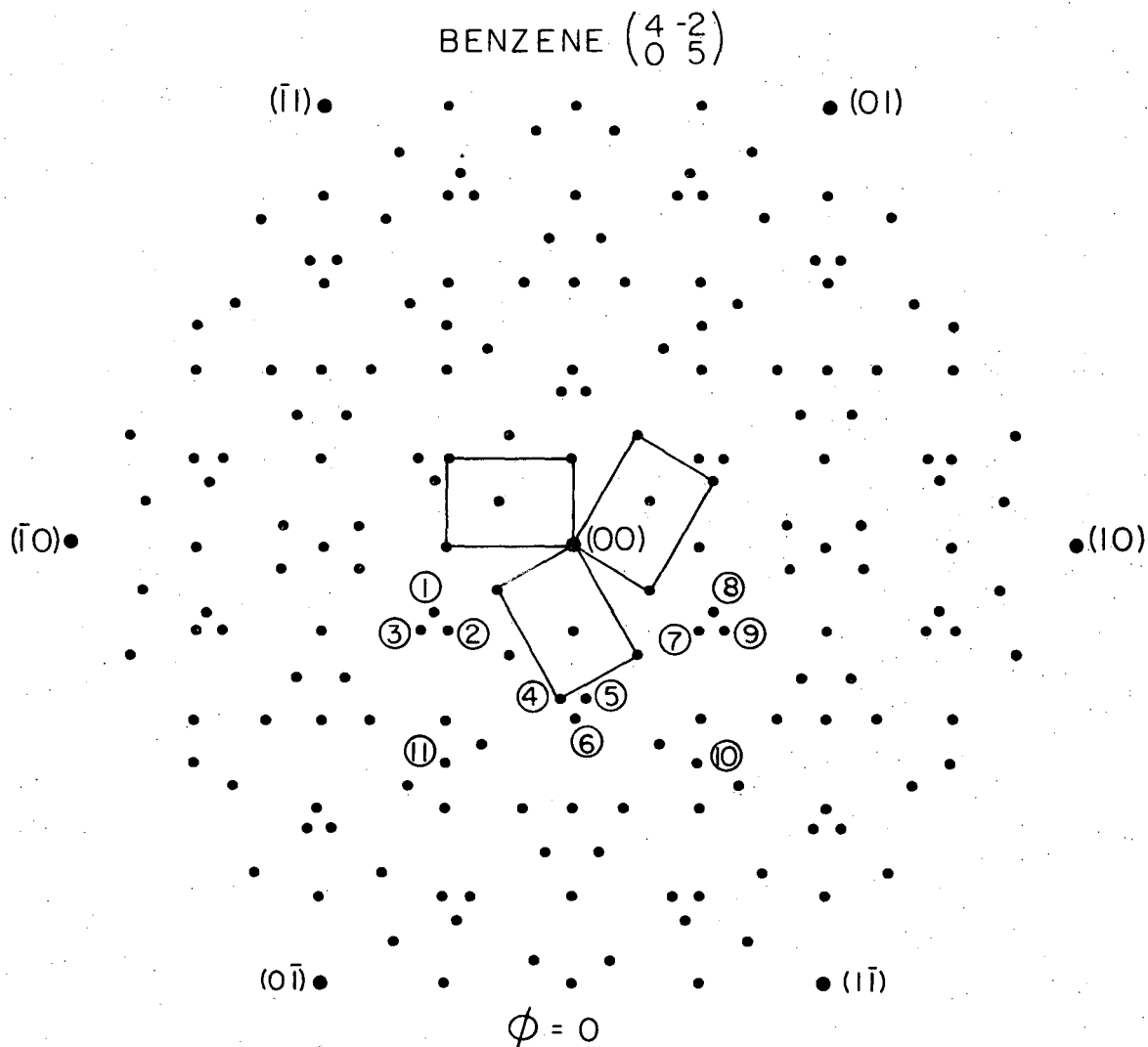
XBL774-5309

fig. 4
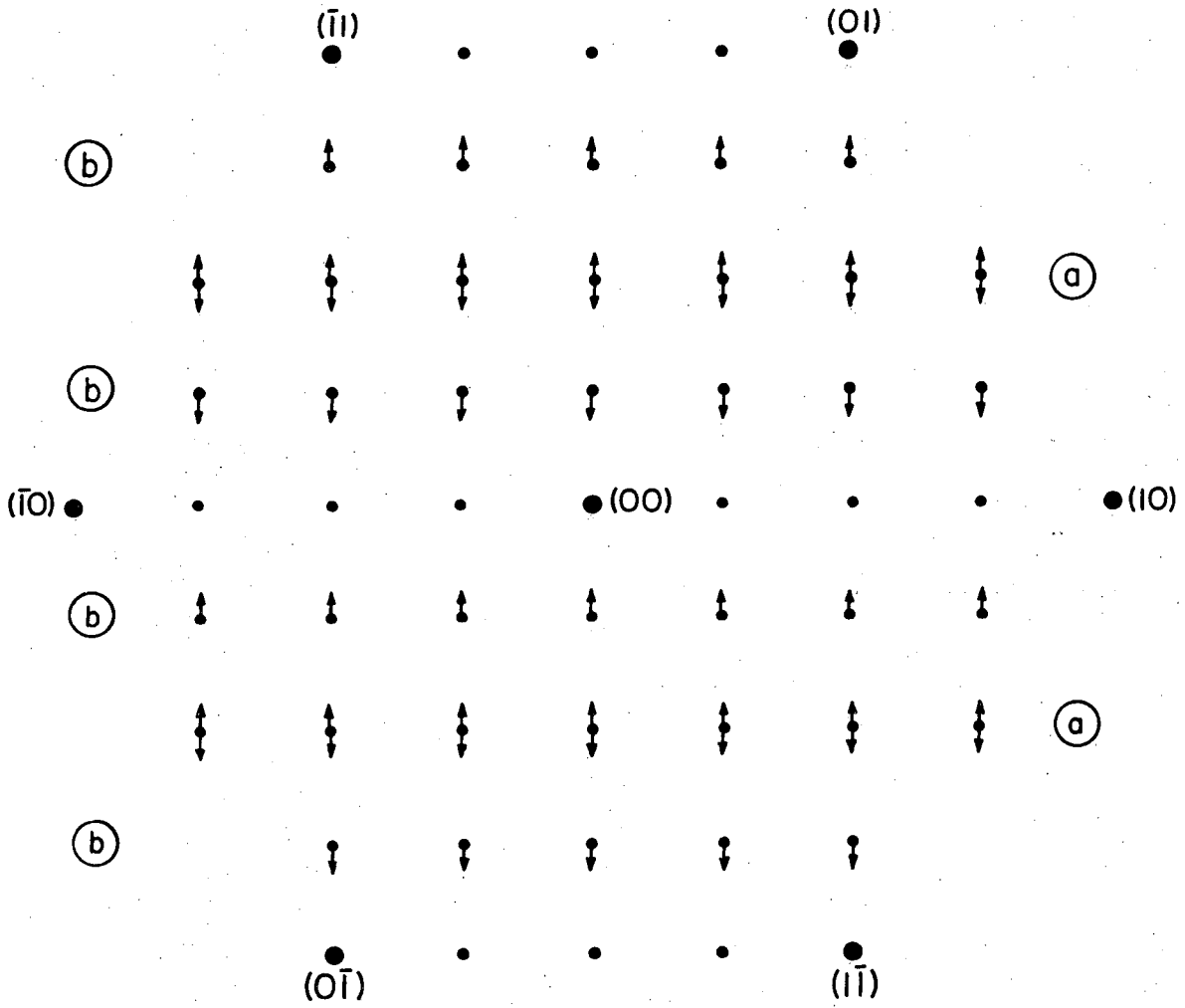
XBL 774-5259

Fig. 5
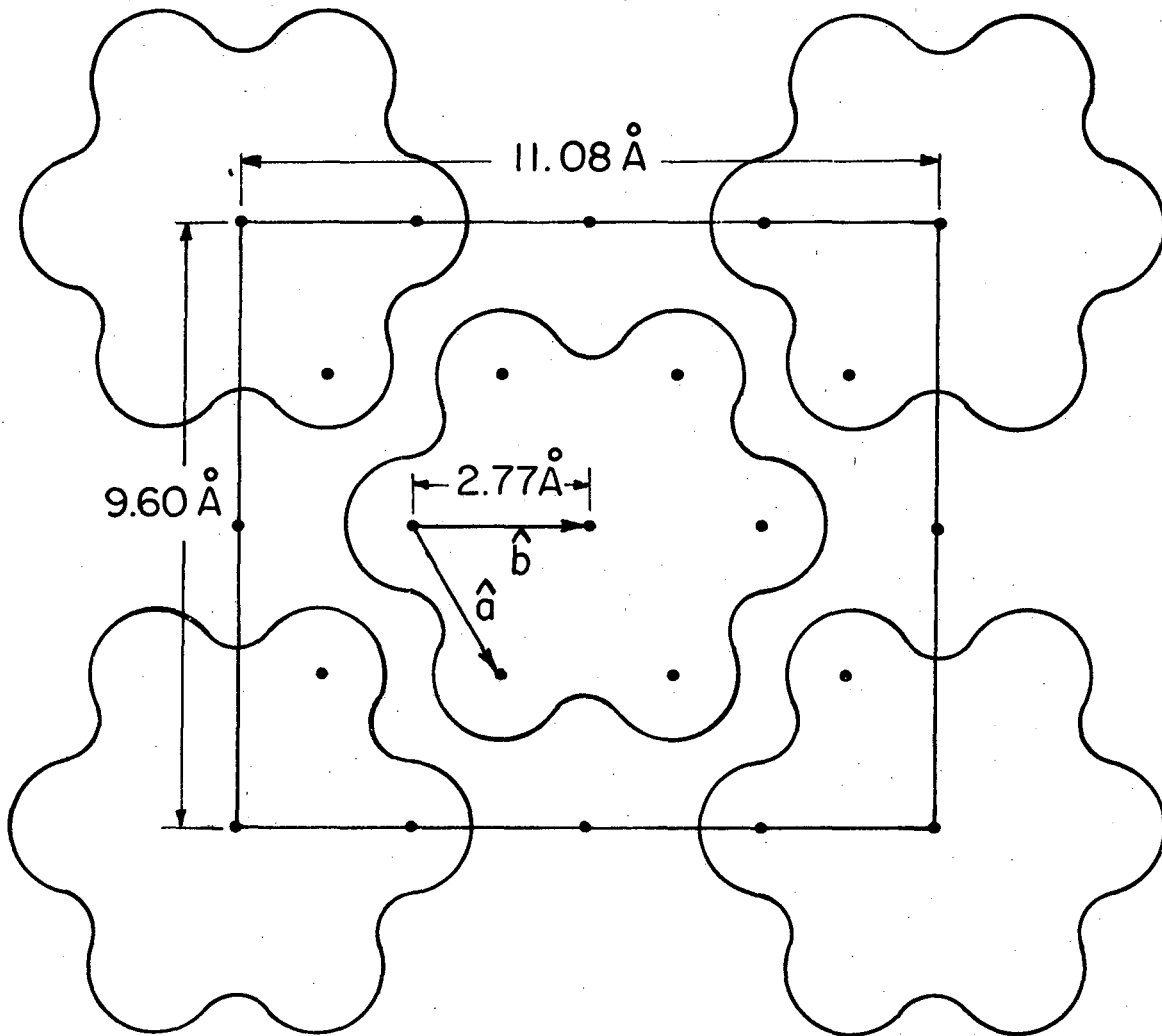
Pt (III) — $\begin{vmatrix} 4\hat{a} & -2\hat{b} \\ 0 & 4\hat{b} \end{vmatrix}$ — Benzene
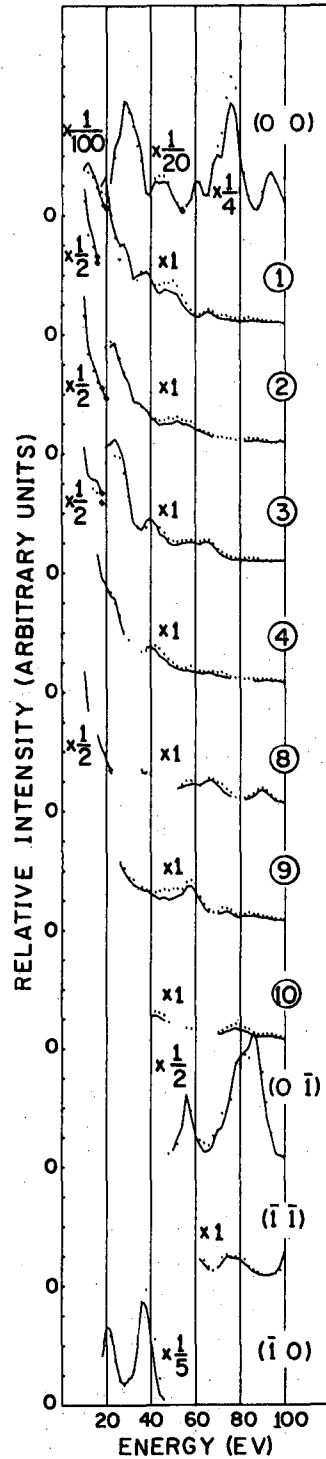
Fig. 6

XBL774-5258

XBL 774-5269

Fig. 1-G1

BENZENE $\begin{pmatrix} 4 & -2 \\ 0 & 4 \end{pmatrix}$

$\theta = 4°$ $\phi = 0$ T=300K

XBL 774-5268

Fig 1-G2

BENZENE $\begin{pmatrix} 4 & -2 \\ 0 & 4 \end{pmatrix}$

$\theta = 10° \ \phi = 0 \ T = 300K$
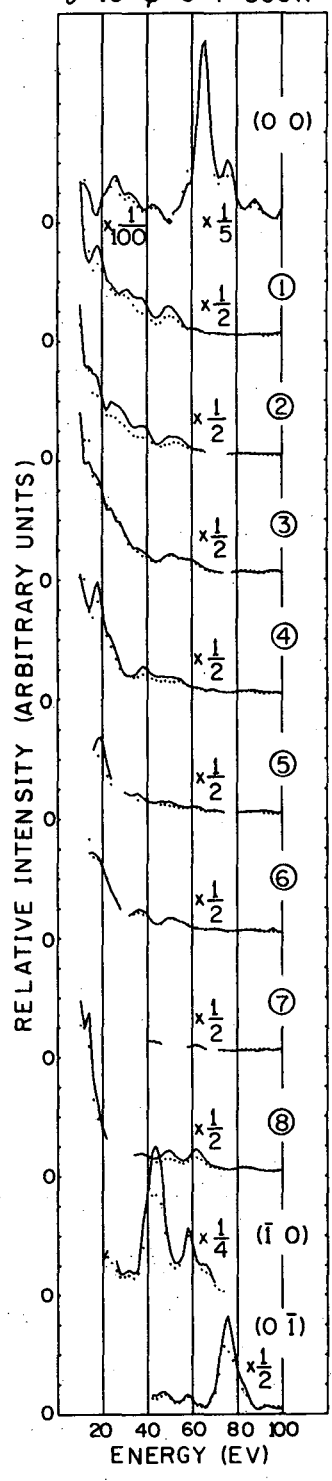
XBL 774-5267

Fig 16-3

BENZENE $\begin{pmatrix} 4 & -2 \\ 0 & 4 \end{pmatrix}$
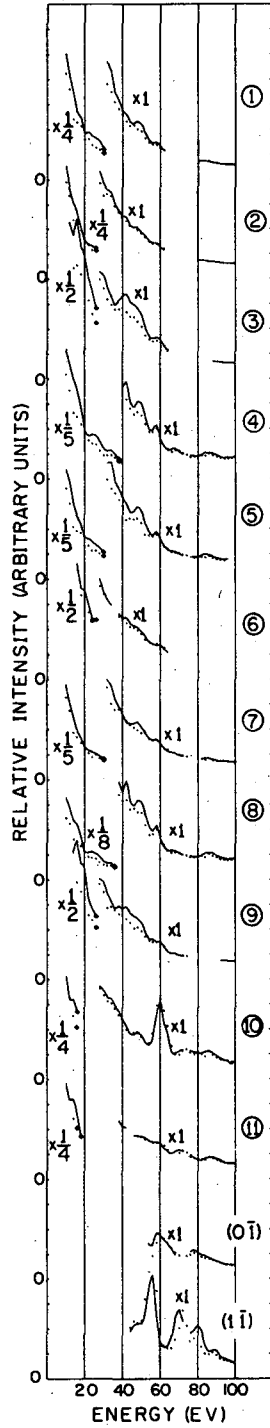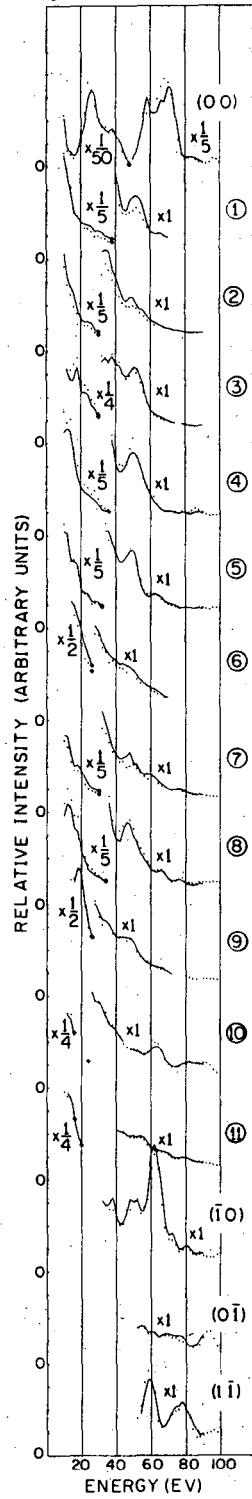
$\theta = 16° \quad \phi = 0 \quad T = 300 \ K$

$x\frac{1}{100}$ $x\frac{1}{20}$ $x\frac{1}{4}$ (0 0)

$x\frac{1}{2}$ $x1$ ①

$x\frac{1}{2}$ $x1$ ②

$x\frac{1}{2}$ $x1$ ③

$x1$ ④

$x\frac{1}{2}$ $x1$ ⑧

$x1$ ⑨

$x1$ ⑩

$x\frac{1}{2}$ (0 $\bar{1}$)

$x1$ ($\bar{1}$ $\bar{1}$)

$x\frac{1}{5}$ ($\bar{1}$ 0)

RELATIVE INTENSITY (ARBITRARY UNITS)

20 40 60 80 100

ENERGY (EV)

XBL 774-5266

Fig 16-4
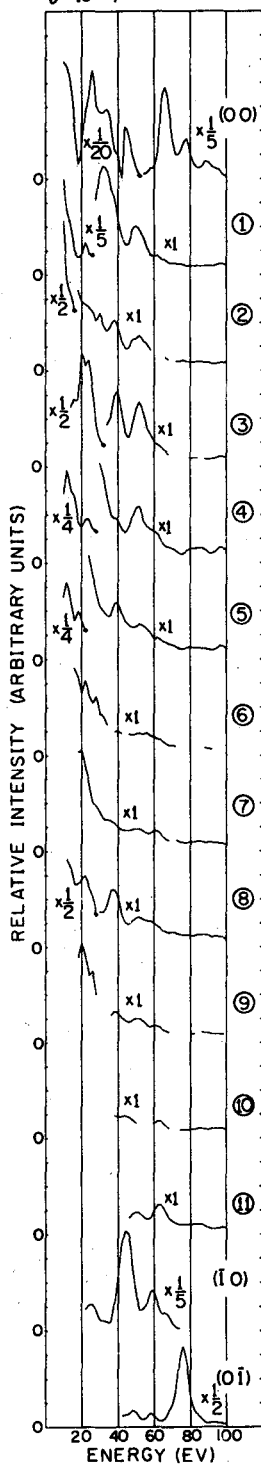
BENZENE $\begin{pmatrix} 4 & -2 \\ 0 & 5 \end{pmatrix}$

$\theta = 0 \quad \phi = 0 \quad T = 300K$

XBL774-5308

Fig 16-5

BENZENE $\begin{pmatrix} 4 & 2 \\ 0 & 5 \end{pmatrix}$

$\theta = 4°$ $\phi = 0$ T = 300 K

XBL 774-5307

$f_{3}/ - G6$

BENZENE $\begin{pmatrix} 4 & -2 \\ 0 & 5 \end{pmatrix}$

$\theta = 10°$ $\phi = 0$ T = 300 K

Fig 1-67

XBL 774-5306

BENZENE $\begin{pmatrix} 4 & -2 \\ 0 & 5 \end{pmatrix}$
$\theta=16°$ $\phi=0$ T=300 K

XBL 774-5305

Fig 1-68